1220 *Inorg. Chem.* **2010**, *49*, 1220–1229
DOI: 10.1021/ic902183c

Inorganic Chemistry
Article

Lithium Furyl and Pyridyl Amidinates as Building Blocks in Coordination Polymers, Ladder and Cage Structures

Sinai Aharonovich,[†] Mark Botoshanski,[†] Ziv Rabinovich,[†] Robert M. Waymouth,[‡] and Moris S. Eisen*[,†]

[†]*Schulich Faculty of Chemistry and Institute of Catalysis Science and Technology, Kyriat Hatechnion, Haifa, 32000, Israel and* [‡]*Department of Chemistry, Stanford University, Stanford, California 94305-5080*

Received November 5, 2009

Lithium *N,N′*-bis(trimethylsilyl)heterocyclic amidinate complexes with 3- and 4-pyridyl and 3-furyl carbon substituents were prepared by addition of the corresponding nitriles to $LiN(SiMe_3)_2$ ($LiNTMS_2$) solution. In the presence of *N,N,N′, N′* tetramethylethylene diamine (TMEDA), both pyridyl amidinates crystallize as coordination polymers with an amidinate-Li-pyridyl backbone. The 4-pyridyl derivative (**7**) creates a linear polymer with amidinate-Li-TMEDA units as side chains, whereas the 3-pyridyl polymer (**6**) has a two-dimensional (2D) network structure in which TMEDA serves as a cross-linker. Solvation of the reaction mixture of 3-furonitrile and $LiNTMS_2$ with TMEDA affords the monomeric 3-furyl amidinate Li TMEDA complex (**3**). Crystals of the Li_2O complex $\{[3\text{-furyl-C-}(NTMS)_2Li]_4 \cdot Li_2O\} \cdot C_7H_8$ (**4**) are obtained from toluene by partial hydrolysis of the unsolvated 3-furyl amidinate (**2**). Degradation of the polymer (**7**) to monomeric units can be achieved by solvation in toluene or by reaction with $TMS_2NLi \cdot$TMEDA that affords crystals of the complex $\{NTMS_2Li \cdot [4\text{-}C_5H_4N\text{—}C(NTMS)_2Li \cdot TMEDA]\}_2 \cdot (NTMS_2Li \cdot TMEDA)$ (**8**). The formation of these aggregates can be rationalized by directed substitution of TMEDA with pyridyl moieties and by the laddering principle.

Introduction

The well documented popularity of the amidinates, $[N(R_1)\text{-}C(R_2)NR_3]^-$, as ancillary ligands in coordination chemistry[1,2] is partially due to their ability to form stable complexes of metals or metalloids spanning the entire periodic table, which can support unusual bonding motifs and reactivity.[1−3] The simplicity of their synthesis from widely available starting materials,[4] and the ability to tailor the amidinate steric and electronic properties by choice of appropriate carbon and nitrogen substituents, constitute further benefits.[2,5−11] Lithium amidinates are used extensively as ligand transfer reagents in the preparation of the aforementioned amidinate complexes, and as synthons in the preparation of various aza-heterocycles,[7,11,12]

*To whom correspondence should be addressed. E-mail: chmoris@tx.technion.ac.il.

(1) (a) Edelmann, F. T. *Adv. Organomet. Chem.* **2008**, *57*, 183–352. (b) Schareina, T.; Kempe, R. Amido ligands in coordination chemistry. In *Synthetic methods of organometallic and inorganic chemistry*; Herrmann, W. A., Ed.; Thieme: Germany, 2002; Vol. *10*, pp 1−41.(c) Kissounko, D. A.; Zabalov, M. V.; Brusova, G. P.; Lemenovskii, D. A. *Russ. Chem. Rev.* **2006**, *75*, 351–374.
(2) Junk, P. C.; Cole, M. L. *Chem. Commun.* **2007**, *16*, 1579–1590.
(3) (a) Wang, J.; Yao, Y.; Zhang, Y.; Shen, Q. *Inorg. Chem.* **2009**, *48*, 744–751. (b) Sun, J.-F.; Chen, S.-J.; Duan, Y.; Li, Y.-Z.; Chen, X.-T.; Xue, Z.-L. *Organometallics* **2009**, *28*, 3088–3092. (c) Wu, Y.-Y.; Yeh, C.-W.; Chan, Z.-K.; Lin, C.-H.; Yang, C.-H.; Chen, J.-D.; Wang, J.-C. *J. Mol. Struct.* **2008**, *890*, 48–56. (d) Sciarone, T. J. J.; Nijhuis, C. A.; Meetsma, A.; Hessen, B. *Organometallics* **2008**, *27*, 2058–2065. (e) Pap, J. S.; DeBeer George, S.; Berry, J. F. *Angew. Chem., Int. Ed.* **2008**, *47*, 10102–10105. (f) Jones, C.; Rose, R. P.; Stasch, A. *J. Chem. Soc., Dalton Trans.* **2008**, 2871–2878. (g) Ge, S.; Meetsma, A.; Hessen, B. *Organometallics* **2008**, *27*, 3131–3135. (h) Donahue, J. P.; Murillo, C. A. *J. Chem. Soc., Dalton Trans.* **2008**, 1547–1551. (i) Cotton, F. A.; Murillo, C. A.; Young, M. D.; Yu, R.; Zhao, Q. *Inorg. Chem.* **2008**, *47*, 219–229. (j) Luo, Y.; Wang, X.; Chen, J.; Luo, C.; Zhang, Y.; Yao, Y. *J. Organomet. Chem.* **2009**, *694*, 1289–1296. (k) Aharonovich, S.; Volkis, V.; Eisen, M. S. *Macromol. Symp.* **2007**, *260*, 165–171. (l) Aharonovich, S.; Botoshanski, M.; Tumanskii, B.; Nomura, K.; Waymouth, R. M.; Eisen, M. S., *J. Chem. Soc., Dalton Trans.* **2010**, submitted for publication.
(4) (a) Ostrowska, K.; Kolasa, A. In *Science of Synthesis*; Charette, A. B., Ed.; Thieme: Stuttgart, Germany, 2005; Vol. *22*, p 379. (b) Ostrowska, K.; Kolasa, A. In *Science of Synthesis*; Charette, A. B., Ed.; Thieme: Stuttgart, Germany, 2005; Vol. *22*, p 489.
(5) Baker, R. J.; Jones, C. *J. Organomet. Chem.* **2006**, *691*, 65–71.
(6) Knapp, C.; Lork, E.; Watson, P. G.; Mews, R. *Inorg. Chem.* **2002**, *41*, 2014–2025.
(7) Volkis, V.; Nelkenbaum, E.; Lisovskii, A.; Hasson, G.; Semiat, R.; Kapon, M.; Botoshansky, M.; Eishen, Y.; Eisen, M. S. *J. Am. Chem. Soc.* **2003**, *125*, 2179–2194.
(8) (a) Schmidt, J. A. R.; Arnold, J. *J. Chem. Soc., Dalton Trans.* **2002**, 3454–3461. (b) Recknagel, A.; Knoesel, F.; Gornitzka, H.; Noltemeyer, M.; Edelmann, F. T.; Behrens, U. *J. Organomet. Chem.* **1991**, *417*, 363–375. (c) Wedler, M.; Knoesel, F.; Pieper, U.; Stalke, D.; Edelmann, F. T. *Chem. Ber.* **1992**, *125*, 2171–2181. (d) Nimitsiriwat, N.; Gibson, V. C.; Marshall, E. L.; Takolpuckdee, P.; Tomov, A. K.; White, A. J. P.; Williams, D. J.; Elsegood, M. R. J.; Dale, S. H. *Inorg. Chem.* **2007**, *46*, 9988–9997.
(9) Schmidt, J. A. R.; Arnold, J. *J. Chem. Soc., Dalton Trans.* **2002**, 2890–2899.
(10) Aharonovich, S.; Kapon, M.; Botoshanski, M.; Eisen, M. S. *Organometallics* **2008**, *27*, 1869–1877.
(11) Aharonovich, S.; Botoshanski, M.; Eisen, M. S. *Inorg. Chem.* **2009**, *48*, 5269–5278.
(12) (a) Boesveld, W. M.; Hitchcock, P. B.; Lappert, M. F. *J. Chem. Soc., Perkin Trans. 1* **2001**, 1103–1108. (b) Knapp, C.; Lork, E.; Borrmann, T.; Stohrer, W.-D.; Mews, R. *Eur. J. Inorg. Chem.* **2003**, 3211–3220. (c) Ma, Y.; Breslin, S.; Keresztes, I.; Lobkovsky, E.; Collum, D. B. *J. Org. Chem.* **2008**, *73*, 9610–9618. (d) Inukai, Y.; Oono, Y.; Sonoda, T.; Kobayashi, H. *Bull. Chem. Soc. Jpn.* **1979**, *52*, 516–520.

Published on Web 12/29/2009

and other valuable organo-nitrogen compounds.[13,14] These applications have motivated, in the past two decades, substantial studies of the structural chemistry of these lithium complexes.

Like in the chemistry of lithium amides and imides,[15] the coordination mode and aggregation degree between the lithium and the amidinate ligand are strongly influenced by the presence of additional ligands, donor solvents, and by the nitrogen and carbon substituents. Thus, a mononuclear, tetrahedral complex is usually obtained in the presence of chelating donors such as TMEDA, having κ^2 chelating amidinate (a, Figure 1).[6,9,10,16] Monochelating donors like ethers or nitriles can lead to aggregation and to formation of di- or trinuclear complexes in which the amidinate moiety bridges two or three lithium atoms through σ (b, Scheme 1) or mixed σ and π donation to the lithium (c, d, Scheme 1).[2,6,13,17−19]

Modification of the electronic properties[11] or the steric bulk of the nitrogen or carbon substituents can both cause the amidinate to adopt different coordination modes. An example for the latter steric effect is given by the group-I metal formamidinates[2] and terphenyl[9] or triptycenyl[5] amidinates. The steric demand of the former ligand, having a hydrogen atom as the carbon substituent, can be manipulated electively via the nitrogen substituents to yield various coordination modes. For the two latter ligands, the extremely bulky carbon substituents force the less common κ^1 coordination mode for the metal in addition to unusual amidinate tautomeric (*E*, *Z*) forms.

In aryl amidinates the type and position of the aromatic ring substituents can result in considerable structural changes, caused mainly by steric effects.[6,7,10,18] In this work lithium *N*,*N*′-bis(trimethylsilyl) amidinates with the sterically similar 3-furyl and 3- and 4-pyridyl carbon substituents were prepared and characterized. In addition we present the effects

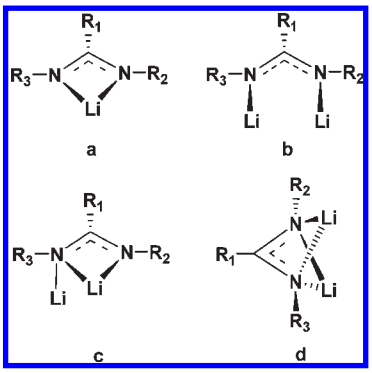

Figure 1. Examples of lithium amidinate coordination modes: (**a**) κ^2; (**b**) κ^1: κ^1 bimetallic bridging; (**c**) κ^2: κ^1 bimetallic bridging and monochelating; (**d**) κ^2: κ^2 bimetallic bridging and bis(chelating).

Scheme 1. Preparation of the *N*,*N*′-bis(trimethylsilyl) Lithium Furyl Amidinate Complexes (**1**−**3**), and the Cage Structure (**4**)

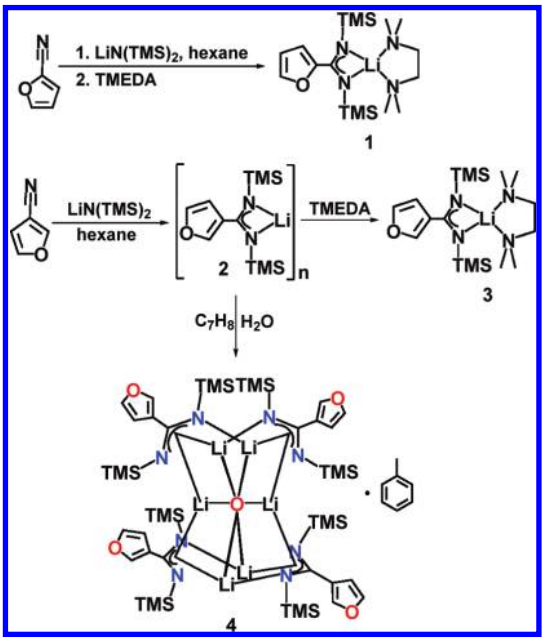

of the type and the position of the pendant ring heteroatom of these new ligands, and also of the previously prepared 2-furyl and 2-pyridyl derivatives,[10] on the lithium amidinate structures, aggregation modes, and reactivity.

Results and Discussion

Synthesis and Reactivity of the Lithium 3-Furyl Amidinate Complexes 2−4. Preparation of the lithium 3-furyl amidinate TMEDA complex (**3**) was found to be more challenging than the isomeric 2-furyl complex (**1**) (Scheme 1).[10] When the synthesis of complex **3** was attempted by the addition of 3-furonitrile to a 0 °C hexane solution of $LiNTMS_2$, similar to the protocol for the preparation of other silylated aryl amidinates,[7,10,19,20] dark brown solids precipitate. This lithium-containing *pyrophoric* material, which presumably originates from deprotonation and/or nucleophilic attack at the 2 or 5 position of the 3-substituted furan ring,[21] is polymeric in

(13) Ong, T.-G.; O'Brien, J. S.; Korobkov, I.; Richeson, D. S. *Organometallics* **2006**, *25*, 4728–4730.
(14) Boesveld, W. M.; Hitchcock, P. B.; Lappert, M. F. *J. Chem. Soc., Dalton Trans.* **1999**, 4041–4046.
(15) (a) Armstrong, D. R.; Barr, D.; Clegg, W.; Mulvey, R. E.; Reed, D.; Snaith, R.; Wade, K. *J. Chem. Soc., Chem. Commun.* **1986**, 869–870. (b) Gregory, K.; Schleyer, P. v. R.; Snaith, R. *Adv. Inorg. Chem.* **1991**, *37*, 47–142. (c) Mulvey, R. E. *Chem. Soc. Rev.* **1991**, *20*, 167–209. (d) Mulvey, R. E. *Chem. Soc. Rev.* **1998**, *27*, 339–346. (e) Downard, A.; Chivers, T. *Eur. J. Inorg. Chem.* **2001**, 2193–2201.
(16) (a) Baldamus, J.; Berghof, C.; Cole, M. L.; Hey-Hawkins, E.; Junk, P. C.; Louis, L. M. *Eur. J. Inorg. Chem.* **2002**, 2878–2884. (b) Dick, D. G.; Edema, J. J. H.; Duchateau, R.; Gambarotta, S. *Inorg. Chem.* **1993**, *32*, 1959–62. (c) Trifonov, A. A.; Lyubov, D. M.; Fedorova, E. A.; Fukin, G. K.; Schumann, H.; Muhle, S.; Hummert, M.; Bochkarev, M. N. *Eur. J. Inorg. Chem.* **2006**, 747–756. (d) Cole, M. L.; Junk, P. C.; Louis, L. M. *J. Chem. Soc., Dalton Trans.* **2002**, 3906–3914.
(17) (a) Barker, J.; Barr, D.; Barnett, N. D. R.; Clegg, W.; Cragg-Hine, I.; Davidson, M. G.; Davies, R. P.; Hodgson, S. M.; Howard, J. A. K.; Kilner, M.; Lehmann, C. W.; Lopez-Solera, I.; Mulvey, R. E.; Raithby, P. R.; Snaith, R. *J. Chem. Soc., Dalton Trans.* **1997**, 951–955. (b) Hitchcock, P. B.; Lappert, M. F.; Merle, P. G. *J. Chem. Soc., Dalton Trans.* **2007**, 585–594. (c) Stalke, D.; Wedler, M.; Edelmann, F. T. *J. Organomet. Chem.* **1992**, *431*, C1–C5. (d) Villiers, C.; Thuery, P.; Ephritikhine, M. *Eur. J. Inorg. Chem.* **2004**, 4624–4632. (e) Richter, J.; Feiling, J.; Schmidt, H.-G.; Noltemeyer, M.; Brueser, W.; Edelmann, F. T. *Z. Anorg. Allg. Chem.* **2004**, *630*, 1269–1275. (f) Hitchcock, P. B.; Lappert, M. F.; Merle, P. G. *Phosphorus, Sulfur Silicon Relat. Elem.* **2001**, *168*−*169*, 363–366. (g) Pang, X.-A.; Yao, Y.-M.; Wang, J.-F.; Sheng, H.-T.; Zhang, Y.; Shen, Q. *Chin. J. Chem.* **2005**, *23*, 1193–1197. (h) Mansfield, N. E.; Coles, M. P.; Hitchcock, P. B. *J. Chem. Soc., Dalton Trans.* **2005**, 2833–2841.
(18) Eisen, M. S.; Kapon, M. *J. Chem. Soc., Dalton Trans.* **1994**, 3507–3510.
(19) Lisovskii, A.; Botoshansky, M.; Eisen, M. S. *J. Chem. Soc., Dalton Trans.* **2001**, 1692–1698.
(20) Edelmann, F. T. *Coord. Chem. Rev.* **1994**, *137*, 403–481.
(21) (a) Divald, S.; Chun, M. C.; Joullie, M. M. *J. Org. Chem.* **1976**, *41*, 2835–2846. (b) Bures, E.; Nieman, J.; Yu, A. S.; Spinazze, P. G.; Bontront, J. -L. J.; Hunt, I. R.; Rauk, A.; Keay, B. A. *J. Org. Chem.* **1997**, *62*, 8750–8759.

Table 1. Crystallographic Data for Complexes **3**, **4**, **6**, **7**, and **8**

	3	**4**	**6**	**7**	**8**
empirical formula	$C_{17}H_{37}LiN_4OSi_2$	$C_{51}H_{92}Li_6N_8O_5Si_8$	$C_{15}H_{30}LiN_4Si_2$	$C_{30}H_{60}Li_2N_8Si_4$	$C_{60}H_{146}Li_5N_{15}Si_{10}$
Fw [g/mol]	376.63	1163.69	329.55	659.1	1393.52
T [K]	240(1)	240(1)	230.0(1)	230.0(1)	230.0(1)
λ [Å]	0.71073	0.71073	0.71073	0.71073	0.71073
crystal system	monoclinic	monoclinic	monoclinic	orthorhombic	monoclinic
space group	$P2_1/n$	$P2_1/c$	$P2_1/n$	$Pbca$	$P2_1/c$
a [Å]	10.546(2)	10.895(2)	11.7590(10)	16.8710(4)	20.7270(5)
b [Å]	13.344(3)	29.046(6)	16.0250(14)	19.9930(5)	24.7440(8)
c [Å]	17.583(3)	22.163(4)	12.6520(14)	25.8950(9)	20.7560(4)
β [deg]	90.70(2)	95.95(2)	117.732(3)	90	114.0900(16)
V [Å^3]	2474.2(8)	6976(2)	2110.3(3)	8734.4(4)	9718.0(4)
Z	4	4	4	8	4
ρ [g/cm^3]	1.011	1.108	1.037	1.002	0.952
μ(Mo Kα) [mm^{-1}]	0.154	0.198	0.169	0.163	0.172
R1, wR2($I > 2\sigma(I)$)	0.0730, 0.2092	0.0568, 0.1365	0.0620, 0.1197	0.0621, 0.1672	0.0685, 0.2007
R1, wR2 (all data)	0.1082, 0.2295	0.1149, 0.1532	0.2170, 0.1450	0.1044, 0.1883	0.1209, 0.2290
GOF on F^2	1.093	1	0.801	1.086	1.013
F(000)	824	2496	716	2864	3064
θ range for data collection [deg.]	1.92 to 25.05	1.40 to 27.52	1.96 to 25.05	1.57 to 23.00	1.08 to 22.98
limiting indices	$0 \le h \le 12$	$0 \le h \le 13$	$-13 \le h \le 14$	$0 \le h \le 18$	$-22 \le h \le 22$
	$0 \le k \le 15$	$0 \le k \le 37$	$-19 \le k \le 17$	$0 \le k \le 21$	$-27 \le k \le 27$
	$-20 \le l \le 20$	$-28 \le l \le 28$	$-15 \le l \le 14$	$0 \le l \le 28$	$-22 \le l \le 22$
reflections collected/unique	18841/4356	70110/15754	6176/3668	6000/6000	26286/13460
R(int)	0.0600	0.0570	0.1158	0.0000	0.0365
completeness to θ_{max} [%]	99.5	98.10	98.20	98.70	99.70
data/restraints /parameters	4356/0/220	15754/0/703	3668/0/229	6000/0/416	13460/0/815
max. diff. peak and hole [e/Å^{-3}]	0.728 and 0.675	0.414 and 0.275	0.178 and 0.224	0.512 and 0.580	0.489 and 0.366

nature, judging from its extremely low solubility in toluene (even after the addition of an excess of TMEDA), which improves in ether or THF. This material reacts rapidly with Me_3SiCl yielding a brown oil with the concomitant precipitation of LiCl. ^{1}H NMR measurements of the starting oligo/poly lithium material or the brown oil product corroborated that in both cases a myriad of compounds are obtained. Only when the synthesis is attempted at −20 °C, amidinate **2** can be extracted with toluene from the dark reaction mixture in an analytically pure isolated yield of 5%. This intermediate (**2**) reacts cleanly with TMEDA to furnish complex **3** in a nearly quantitative isolated yield (>90%). The addition of 3-furonitrile to the $LiNTMS_2$ solution at lower temperatures (−40 °C) results in instantaneous formation of white solids, presumably because of precipitation of $LiNTMS_2$-nitrile[10] or $LiNTMS_2$-nitrile-amidinate[19] polynuclear complexes, which reacts only at higher temperatures. Attempts to improve this yield by conducting the reaction in the presence of more polar or coordinative solvents such as TMEDA, ether, or tetrahydrofuran (THF) were hampered by the higher solubility of the other lithiated products in these solvents (vide supra), which complicates the isolation of the lithium amidinate. Several crystals of the amidinate cage complex **4**, the third example of such a structure,[22,23] were isolated from the toluene/hexane mixture used to purify compound **2**. A controlled hydrolysis of **2** provides complex **4** in a 33% isolated yield, indicating that the source of the central oxide anion was the adventitious water present in the washing solvents.

Solid State Structure of the Mononuclear Lithium Amidinate Complex 3 and the Hexalithium Cage 4. Crystallographic data and structure refinement details for complex **3** and selected bond lengths and angles are presented in Tables 1 and 2, respectively. The intramolecular solid state structure of complex **3** (Figure 2), having a distorted tetrahedral environment for the lithium atom with a predominantly κ^2 chelating amidinate and TMEDA ligands, is similar to the structures of other lithium arylamidinate TMEDA complexes.[6,7,10] Additional similarities of complex **3** to the aforementioned mononuclear amidinates are the near perpendicularity of the 3-furyl ring and the amidinate plane (80.5°), and the Li-N-C-N dihedral angle in this complex (7.8°), which demonstrates a slight slippage of the lithium atom toward pi bonding with the amidinate ligand. We have previously shown that this lithium slippage is associated with the formation of intermolecular interactions in the lattice between the negatively charged NCN core and the partially positively charged moieties such as TMEDA methyls. These interactions result in the formation of dimers or higher aggregates and in shortening of the intermolecular distance in these complexes in nearly 1 Å as compared to complexes with no such interactions.[10] The similarity of the value of this dihedral angle in complex **3** and complexes

Table 2. Key Bond Lengths [Å] and Angles [deg] for Complex **3**

bond lengths		bond angles	
Si(1)−N(1)	1.707(3)	C(1)−N(1)−Si(1)	131.7(2)
Si(2)−N(2)	1.703(3)	C(1)−N(1)−Li(1)	85.0(2)
N(1)−C(1)	1.318(4)	Si(1)−N(1)−Li(1)	142.7(2)
N(1)−Li(1)	2.029(6)	C(1)−N(2)−Si(2)	132.0(2)
N(2)−C(1)	1.324(4)	C(1)−N(2)−Li(1)	85.2(2)
N(2)−Li(1)	2.022(6)	Si(2)−N(2)−Li(1)	142.0(2)
N(3)−Li(1)	2.102(6)	N(1)−C(1)−N(2)	120.2(3)
N(4)−Li(1)	2.102(7)	N(2)−Li(1)−N(1)	68.9(2)
C(1)−C(2)	1.500(4)	N(2)−Li(1)−N(3)	133.1(4)
contact distance		N(1)−Li(1)−N(3)	129.4(3)
N(1)····C(15)	3.987	N(2)−Li(1)−N(4)	120.6(3)
dihedral angle		N(1)−Li(1)−N(4)	124.1(3)
Li(1)−N(1)−C(1)−N(2)	7.80	N(3)−Li(1)−N(4)	86.5(2)

(22) Chivers, T.; Downard, A.; Yap, G. P. A. *J. Chem. Soc., Dalton Trans.* **1998**, 2603–2606.
(23) Knapp, C.; Lork, E.; Mews, R. *Z. Anorg. Allg. Chem.* **2003**, *629*, 1511–1514.

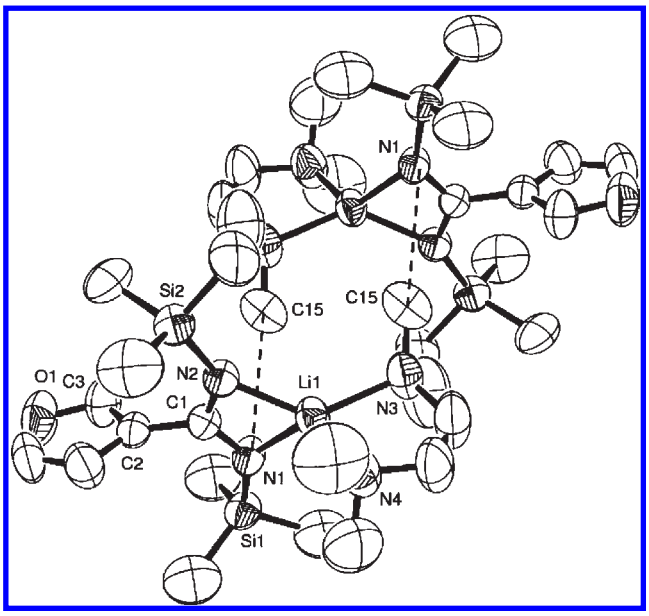

Figure 2. ORTEP diagram of complex **3**, showing a dimer (50% thermal ellipsoids). Dotted line represents the C−N interactions forming the dimers. Hydrogen atoms are omitted for clarity.

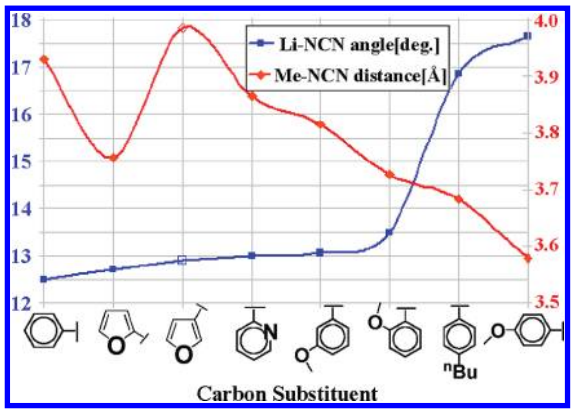

Figure 3. Me···$N_{(amidinate)}$ intermolecular distances (♦, Å) and the Li−NCN dihedral angle (■, degrees) in several bis-silylated lithium aryl amidinates with dimeric or polymeric supramolecular structures. Complex **3** (this work) is labeled with empty marker signs (□, ◊).

that adopt a dimeric supramolecular structure (Figure 3) is indeed accompanied by a dimeric supramolecular structure for complex **3**, formed by the weak interaction between a methyl group of the TMEDA moiety and a nitrogen atom from the NCN core (N(1)····C(15) = 3.987 Å). To the best of our knowledge, Compound **3** is the complex with the weakest intermolecular interactions that still retains the dimeric structure.

Crystallographic data and structure refinement details for complex **4** and selected bond lengths and angles are presented in Tables 1 and 3, respectively.

Complex **4** crystallizes with one molecule of toluene, as confirmed by X-ray diffraction studies. This lattice toluene molecule is lost easily upon separation of the crystals from the mother liquor (hexane-toluene), as supported by the substoichiometric amount of toluene found in the ^{1}H NMR spectrum of dissolved single crystals of **4**, and by the crumbling of the crystals of **4** to a white powder when left overnight in a dry Schlenk vessel inside the glovebox.

In the solid state, a molecule of complex **4** (Figure 4) contains two types of lithium atoms. The first type is found in 4 units of lithium 3-furyl amidinates, which are arranged as 2 dimers in a twisted eight membered dilithium metallacycles. The 2 lithium atoms of the second type are a part of a linear Li_2O unit (the Li(5)−O(5)−Li(2) angle is 176.8°) which is sandwiched between the rings. The 2 types of lithium environments are differentiated by their Li−O bond lengths (mean values of 1.804 ± 0.004 Å and 1.884 ± 0.004 Å for the Li_2O unit and the other ring lithium atoms, respectively), and by their bonding with the amidinate backbone. Each lithium atom in each ring is predominantly σ bonded to a nitrogen from one amidinate ligand (the range of the Li−NCN dihedral for this bond is 1.78°−14.12°), and also π bonded to the other amidinate ligand in the ring (the Li−NCN dihedral angle range for this bond is 31.00°−38.05°). Each of the Li_2O lithium atoms, on the other hand, is π bonded to two amidinate units from the two rings (the Li−NCN dihedral angle range here is 32.23°−42.17°). Overall, each amidinate ligand coordinates 3 lithium atoms in a μ_3: κ^3: κ^3: κ^1 fashion. For example, the amidinate ligand with the N(1), C(1), and N(2) atoms is κ^3 bonded to Li(1) and Li(2) and κ^1 bonded to Li(3). It is important to point out that the amidinate is not disposed symmetrically when coordinated to Li(1) or Li(2). The bonds of these lithium atoms to N(2) are much shorter (typically by about 0.6 Å) than to N(1) and C(1) which are bonded almost equidistant. This mode of coordination suggests that the "π bonding amidinate" can be more accurately described as being κ^1 bonding by N(2) and κ^2 bonding by the C(1)−N(1) double bond. The electron deficient cage structure, which includes the weak κ^2 - C=N π interactions, probably owes its existence, despite the presence of the Lewis basic oxygen atoms of the 3-furyl rings, to chelate effects.

The ^{7}Li NMR spectrum of a toluene-d_8 solution of complex **4** at room temperature shows only one signal for the lithium atoms, suggesting that in solution the complex is fluxional and scrambling between the lithium atoms is rapid at this temperature. Interestingly, in the room temperature ^{7}Li NMR spectrum of the complex reported by Chivers and co-workers[22] two lithium resonances were detected with different intensities, indicating the rigidity of the latter structure (Figure 5).

Synthesis and Structure of the Polymeric 3- and 4-Pyridyl Amidinates 6 and 7. When toluene solutions of 3- or 4-cyanopyridine and $LiNTMS_2$ are mixed, a white suspension is obtained after 12 h. Unlike other lithium amidinates,[10] addition of TMEDA in a slight excess (1.4 equiv) to this suspension does not result in a clear solution, as expected for the formation of mononuclear TMEDA lithium amidinates. Full solubility of the solids was only achieved after the addition of about 5 equiv of TMEDA. Slow removal of the volatiles from these solutions allowed the isolation of complexes **6** or **7** as colorless crystals (Scheme 2).

Crystallographic data and structure refinement details for complex **6** and selected bond lengths and angles are presented in Tables 1 and 4, respectively.

In the crystalline lattice of complex **6** (Figure 6), each lithium atom has a distorted tetrahedral environment with a κ^2-chelating amidinate, whereas the two other

Table 3. Selected Bond Lengths [Å] and Angles [deg] for Complex **4**

Bond Lengths

O(5)−Li(2)	1.800(4)	N(1)−Li(3)	2.132(4)	N(5)−Li(2)	2.069(4)
O(5)−Li(5)	1.808(4)	N(2)−Li(2)	2.083(4)	N(5)−Li(6)	2.096(4)
O(5)−Li(6)	1.877(4)	N(2)−Li(1)	2.118(4)	N(6)−Li(4)	2.146(4)
O(5)−Li(3)	1.879(4)	N(3)−Li(5)	2.078(4)	N(7)−Li(5)	2.094(4)
O(5)−Li(1)	1.888(4)	N(3)−Li(4)	2.104(4)	N(7)−Li(3)	2.108(4)
O(5)−Li(4)	1.890(4)	N(4)−Li(6)	2.126(4)	N(8)−Li(1)	2.125(4)

Bond and Dihedral Angles

Li(2)−N(2)−Li(1)	71.32(15)	Li(2)−O(5)−Li(5)	176.8(2)
Li(5)−N(3)−Li(4)	72.70(16)	O(5)−Li(3)−N(7)	100.99(19)
Li(5)−N(7)−Li(3)	71.52(16)	Li(5)−N(7)−C(34)−N(8)	34.23
O(5)−Li(1)−N(2)	100.52(18)	Li(1)−N(2)−C(1)−N(1)	31.00
O(5)−Li(1)−N(8)	106.46(18)	Li(2)−N(2)−C(1)−N(1)	40.84
N(2)−Li(1)−N(8)	142.5(2)	Li(3)−N(1)−C(1)−N(2)	3.07
O(5)−Li(2)−N(5)	104.37(19)	Li(5)−N(3)−C(12)−N(4)	42.17
N(5)−Li(2)−N(2)	150.5(2)	Li(4)−N(3)−C(12)−N(4)	31.43
Li(2)−O(5)−Li(6)	83.17(18)	Li(6)−N(4)−C(12)−N(3)	1.78
N(3)−Li(4)−N(6)	144.5(2)	Li(2)−N(5)−C(23)−N(6)	40.31
N(3)−Li(5)−N(7)	152.1(2)	Li(6)−N(5)−C(23)−N(6)	32.76
N(5)−Li(6)−N(4)	137.9(2)	Li(4)−N(6)−C(23)−N(5)	9.26
Li(5)−O(5)−Li(4)	84.16(18)	Li(1)−N(8)−C(34)−N(7)	14.12
N(7)−Li(3)−N(1)	139.6(2)	Li(3)−N(7)−C(34)−N(8)	38.05

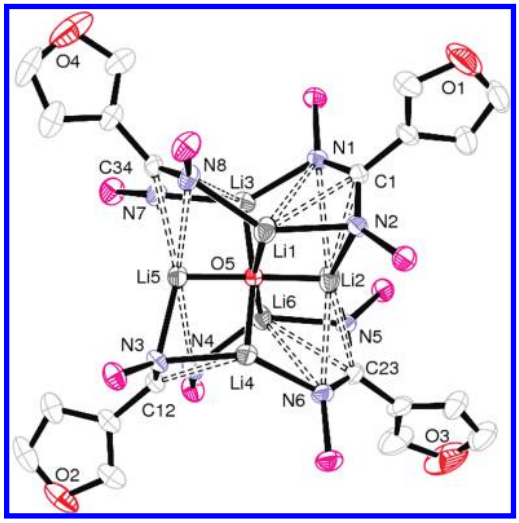

Figure 4. ORTEP diagram of the molecular structure of the cage complex (**4**) (40% thermal ellipsoids). Oxygen, nitrogen, lithium, and silicon atoms are colored red, blue, gray, and pink, respectively. Toluene molecule of crystallization, methyl groups on silicon and hydrogen atoms are omitted for clarity. Dashed bonds represent weaker π interactions.

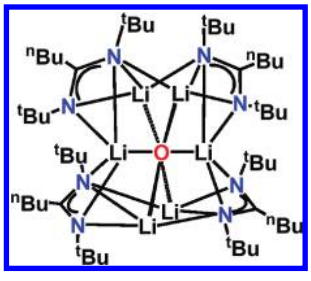

Figure 5. Schematic representation of the cage structure reported by Chivers and co-workers.[22]

bonds are to nitrogen atoms of a TMEDA and a pyridyl ring from an adjacent amidinate fragment. The Li−N(2) bond (2.063 ± 0.007 Å) is slightly shorter than the Li−N(4) bond (2.108 ± 0.008 Å), suggesting that the Li−N interaction with the pyridyl nitrogen is stronger as

Scheme 2. Preparation of the *N*,*N*′-bis(trimethylsilyl) Lithium Pyridylamidinate TMEDA Complexes **5**−**7** from the 3 Isomeric Cyanopyridines

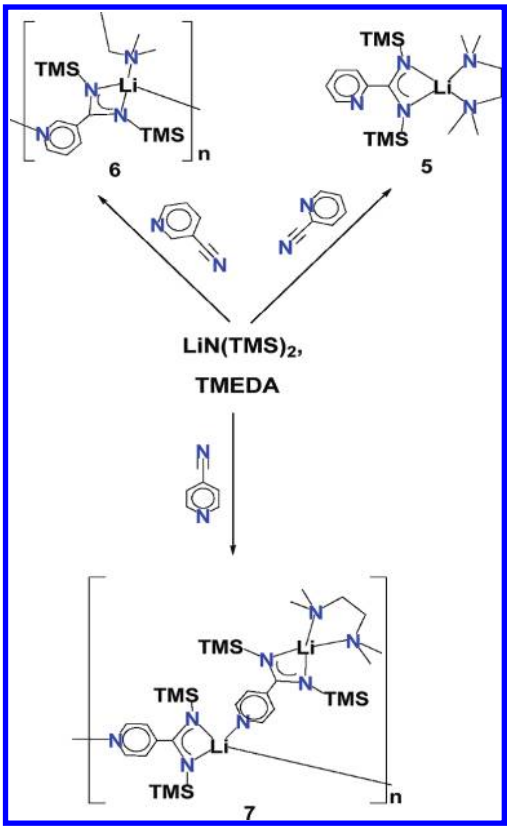

compared to its TMEDA counterpart. The lattice is composed of a two-dimensional (2D) network which consists of $[Li(3\text{-}C_5H_4N)C(NSiMe_3)_2]_n$ chains cross-linked by TMEDA (^{1}H NMR spectrum of this complex shows a 1:2 molar ratio between TMEDA and the amidinate ligand). The cross-linkage between 2 neighboring chains occurs at every second lithium atom, yielding a quasi-syndiotactic stereochemistry at the lithium centers.

Table 4. Selected Bond Lengths [Å] and Angles [deg] for Complex **6**

Bond Lengths					
Si(1)−N(1)	1.692(3)	N(1)−Li(1)	2.092(7)	N(3)−Li(1)	2.046(8)
Si(2)−N(3)	1.696(3)	N(2)−Li(1)	2.063(7)	N(4)−Li(1)	2.108(8)
N(1)−C(4)	1.329(5)	N(3)−C(4)	1.338(4)	C(4)−C(5)	1.502(5)

Bond and Dihedral Angles			
C(4)−N(1)−Si(1)	131.7(3)	N(3)−Li(1)−N(2)	116.5(4)
C(4)−N(1)−Li(1)	84.2(3)	N(3)−Li(1)−N(1)	68.4(3)
Si(1)−N(1)−Li(1)	143.9(3)	N(2)−Li(1)−N(1)	125.6(4)
C(4)−N(3)−Si(2)	131.3(3)	N(3)−Li(1)−N(4)	117.6(3)
C(4)−N(3)−Li(1)	85.9(3)	N(2)−Li(1)−N(4)	111.8(4)
Si(2)−N(3)−Li(1)	142.4(3)	N(1)−Li(1)−N(4)	111.1(3)
N(1)−C(4)−N(3)	121.4(4)	Li(1)−N(1)−C(4)−N(3)	3.9

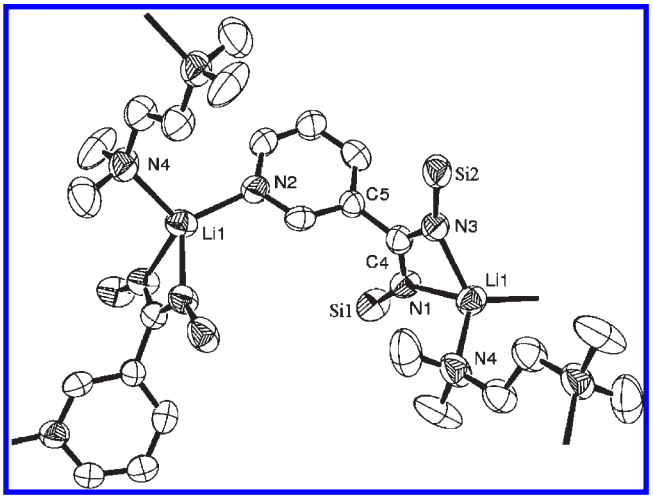

Figure 6. ORTEP diagram of the molecular structure of a segment of the polymer **6** (50% thermal ellipsoids), showing the quasi-syndiotactic stereochemistry at the lithium centers and the TMEDA cross-linkage. Methyl groups on silicon and hydrogen atoms are omitted for clarity.

Crystallographic data and structure refinement details for complex **7** and selected bond lengths and angles are presented in Tables 1 and 5, respectively. The crystalline lattice of the polymeric complex **7** (Figure 7) is composed of linear chains which consist of the lithium 4-pyridyl amidinate motif and TMEDA fragments in a 2:1 molar ratio. Two different kinds of lithium coordination environment exist in complex **7**: backbone, and side chain (Li1 and Li2, respectively, in Figure 6). While both kinds of lithium atoms have a distorted tetrahedral environment with a κ^2 chelating amidinate, the side chain lithium is coordinated by a chelating TMEDA ligand, whereas in the backbone lithium the two other coordination sites are taken by pyridyl nitrogen atoms, one from an adjacent amidinate fragment, and the other from a side chain moiety.

In a similar manner to complex **6**, the side chain lithium amidinate TMEDA units adopt a quasi-syndiotactic stereoarrangement, and the Li−N_{py} bonds (Li1−N4 = 2.085 ± 0.007, Li1−N2 = 2.049 ± 0.006 Å) are slightly shorter than the Li−N_{TMEDA} bonds (Li2−N7 = 2.114 ± 0.007, Li2−N8 = 2.110 ± 0.008 Å). Interestingly, the extent of slippage of the backbone lithium atom from the NCN plane is larger in comparison to its side chain counterpart (Li(1)−N(1)−C(4)−N(3) = 13.1°, as compared to Li(2)−N(5)−C(18)−N(6) = 1.1°). This slippage

Table 5. Key Bond Lengths [Å] and Angles [deg] for Complex **7**

bond angles		bond lengths	
N(1)−C(4)	1.316(5)	C(4)−N(1)−Li(1)	84.0(3)
N(1)−Li(1)	2.056(6)	C(4)−N(3)−Li(1)	84.7(3)
N(2)−Li(1)	2.049(6)	C(18)−N(5)−Li(2)	83.9(3)
N(3)−C(4)	1.328(5)	C(18)−N(6)−Li(2)	85.0(3)
N(3)−Li(1)	2.031(7)	N(1)−C(4)−N(3)	121.0(3)
N(4)−Li(1)	2.085(7)	N(5)−C(18)−N(6)	121.3(3)
N(5)−C(18)	1.329(5)	N(3)−Li(1)−N(2)	127.5(4)
N(5)−Li(2)	2.042(8)	N(3)−Li(1)−N(1)	68.6(2)
N(6)−C(18)	1.331(5)	N(2)−Li(1)−N(1)	131.5(4)
N(6)−Li(2)	2.015(7)	N(3)−Li(1)−N(4)	111.0(3)
N(7)−Li(2)	2.114(7)	N(2)−Li(1)−N(4)	98.2(3)
N(8)−Li(2)	2.110(8)	N(1)−Li(1)−N(4)	119.2(3)
C(4)−C(5)	1.507(5)	N(6)−Li(2)−N(5)	69.7(3)
C(15)−C(18)	1.499(5)	N(6)−Li(2)−N(8)	127.5(4)
dihedral angles		N(5)−Li(2)−N(8)	126.3(4)
Li(1)−N(1)−C(4)−N(3)	13.1	N(6)−Li(2)−N(7)	124.3(4)
Li(2)−N(5)−C(18)−N(6)	1.1	N(5)−Li(2)−N(7)	129.0(4)
contact distance		N(8)−Li(2)−N(7)	86.3(3)
C(28)····N(3)	3.911		

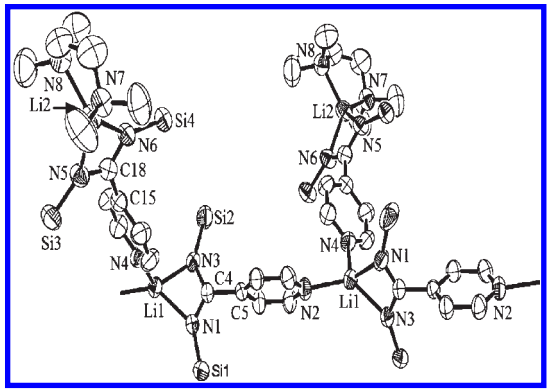

Figure 7. ORTEP diagram of the molecular structure of two repeating units of the polymer **7** (50% thermal ellipsoids), showing the quasi-syndiotactic stereochemistry at the lithium center. Methyl groups on silicon and hydrogen atoms are omitted for clarity.

is a result of the intermolecular packing interaction between the methyl groups of the TMEDA motif and the NCN backbone from two different chains (C(28)····N(3) = 3.911 Å).

Degradation of the Polymeric Lithium 4-Pyridyl Amidinate 7. Not surprisingly, the heavily cross-linked complex **6** has a negligible solubility in toluene, and high solubility in THF, which can facilitate its degradation to smaller aggregates. Complex **7**, on the other hand, has a more pronounced solubility in toluene. The almost clear

Scheme 3. Various Lithium 4-Pyridyl Amidinate Aggregates[a]

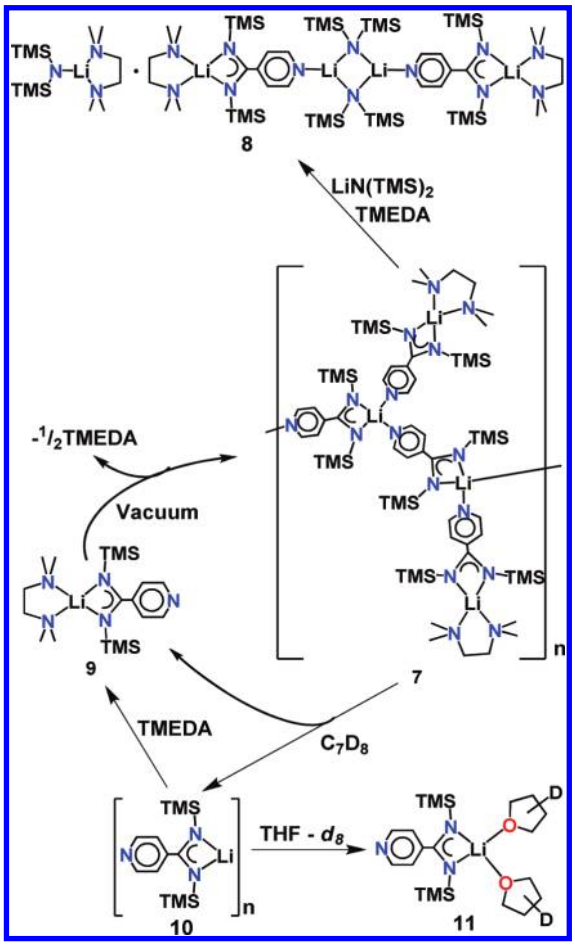

[a] Degradation of the linear polymer **7** to the tetralithium complex **8** by reaction with $LiNTMS_2 \cdot TMEDA$, and to complexes **9** and **10** in toluene. Solvation of the latter complex in THF yields complex **11**.

toluene-d_8 solution of **7** gets turbid shortly after its preparation because of precipitation of an unsolvated lithium amidinate intermediate (**10**, Scheme 3). The ^{1}H NMR spectrum of the remaining solution shows that it contains species with a 1:1 TMEDA/amidinate ratio, plausibly a monomeric TMEDA adduct, as exhibited in complex **9**.

Interestingly, slow removal of the solvents from this solution in vacuum regenerates the polymeric complex **7**, as corroborated by X-ray diffraction studies. This complex is obtained because of loss of 0.5 equiv of TMEDA, aided by the known toluene-TMEDA azeotrope. The assignment of **10** to an unsolvated amidinate species is supported by the presence of a large TMS signal in its THF-d_8 ^{1}H NMR spectrum, which is accompanied by only traces of TMEDA, indicating that a TMEDA free THF adduct, such as **11**, is obtained by the solvation of intermediate **10** in THF.

Another degradation pathway of complex **7** was found when it was dissolved in a mixture of TMEDA and toluene with an excess of $LiNTMS_2$, producing complex **8** in high yields. Crystallographic data and structure refinement details and selected bond lengths and angles for complex **8** are presented in Tables 1 and 6, respectively. The solid state structure of complex **8** (Figure 8) contains a dimeric $[LiNTMS_2]_2$ core which is connected

Table 6. Key Bond Lengths [Å] and Angles [deg] for Complex **8**

bond lengths		bond angles	
N(1)−Li(1)	1.891 (9)	N(1)−Li(1)−N(3)	140.5(5)
N(2)−Li(1)	2.075 (10)	N(1)−Li(1)−N(2)	132.4(5)
N(3)−Li(1)	2.069 (9)	N(3)−Li(1)−N(2)	86.5(4)
N(4)−Li(2)	2.094 (9)	N(5)−Li(2)−N(4)	87.5(3)
N(5)−Li(2)	2.081 (8)	N(7)−Li(2)−N(6)	69.3(3)
N(6)−C(22)	1.325 (4)	N(8)−Li(3)−N(10)	129.6(4)
N(6)−Li(2)	2.038 (7)	N(8)−Li(3)−N(9)	124.3(3)
N(7)−C(22)	1.313 (5)	N(10)−Li(3)−N(9)	106.0(3)
N(7)−Li(2)	2.014 (7)	Li(4)−N(9)−Li(3)	74.1(3)
N(8)−Li(3)	2.025 (7)	Li(3)−N(10)−Li(4)	73.8(3)
N(9)−Li(4)	2.022 (7)	N(9)−Li(4)−N(11)	128.0(4)
N(9)−Li(3)	2.035 (8)	N(9)−Li(4)−N(10)	106.1(3)
N(10)−Li(3)	2.032 (7)	N(11)−Li(4)−N(10)	125.9(3)
N(10)−Li(4)	2.044 (8)	N(13)−Li(5)−N(12)	68.8(2)
N(11)−Li(4)	2.025 (7)	N(15)−Li(5)−N(14)	87.5(3)
N(12)−C(48)	1.317(5)	dihedral angles	
N(12)−Li(5)	2.043 (7)	Li(2)−N(6)−C(22)−N(7)	3.7
N(13)−C(48)	1.323 (4)	N(6)−C(22)−C(26)−C(27)	85.0
N(13)−Li(5)	2.025 (7)	Li(3)−N(9)−Li(4)−N(10)	0.4
N(14)−Li(5)	2.085 (8)	N(12)−C(48)−C(45)−C(46)	86.1
N(15)−Li(5)	2.076 (7)	Li(5)−N(12)−C(48)−N(13)	1.0

to two monomeric lithium 4-pyridyl amidinate TMEDA units through their pyridyl nitrogen atoms. The central Li−N−Li−N metallacycle is a very common structural motif and can be found in many complexes of $LiNTMS_2$ in which the lithium atoms are bonded to various donor ligands.[10,24]

The structure of complex **8** supports the notion that in rich TMEDA solutions the pyridyl amidinates exist as mononuclear complexes, and that the polymerization is reversible, and can be prevented by binding of the pyridyl nitrogen to a Lewis acid ($LiNTMS_2$), which obstructs the pyridyl ability to substitute a TMEDA nitrogen. Fascinatingly, **8** co-crystallizes with a separate $LiNTMS_2 \cdot$ TMEDA molecule.

Formation of the Polymeric Lithium 3- and 4-Pyridyl Amidinates. In polymers **6** and **7**, and in the tetralithium complex **8** the pyridyl amidinate ligand can be regarded as tridentate (bidentate chelating at the amidinate NCN core and bridging through the pyridyl nitrogen). The aggregation, which takes place in the presence of the chelating TMEDA, is affected by steric factors, as demonstrated by the 2-pyridyl complex **5** (Scheme 2) that does not aggregate and can be crystallized in the monomeric

(24) (a) Boyle, T. J.; Scott, B. L. *Acta Crystallogr., Sect. C* **1998**, C54. (b) Engelhardt, L. M.; Jolly, B. S.; Junk, P. C.; Raston, C. L.; Skelton, B. W.; White, A. H. *Aust. J. Chem.* **1986**, *39*, 1337. (c) Romesberg, F. E.; Bernstein, M. P.; Gilchrist, J. H.; Harrison, A. T.; Fuller, D. J.; Collum, D. B. *J. Am. Chem. Soc.* **1993**, *115*, 3475. (d) Lucht, B. L.; Collum, D. B. *J. Am. Chem. Soc.* **1995**, *117*, 9863. (e) Lucht, B. L.; Collum, D. B. *J. Am. Chem. Soc.* **1996**, *118*, 3529. (f) Henderson, K. W.; Dorigo, A. E.; Liu, Q.-Y.; Williard, P. G. *J. Am. Chem. Soc.* **1997**, *119*, 11855. (g) Hartung, M.; Guinther, H.; Amoureux, J.-P.; Fernandez, C. *Magn. Reson. Chem.* **1998**, *36*, S61. (h) Williard, P. G.; Liu, Q. Y.; Lochmann, L. *J. Am. Chem. Soc.* **1992**, *114*, 348. (i) Armstrong, D. R.; Davies, R. P.; Dunbar, L.; Raithby, P. R.; Snaith, R.; Wheatley, A. E. H. *Phosphorus, Sulfur Silicon Relat. Elem.* **1997**, *124 & 125*, 51. (j) Lucht, B. L.; Collum, D. B. *J. Am. Chem. Soc.* **1996**, *118*, 2217. (k) Henderson, K. W.; Williard, P. G. *Organometallics* **1999**, *18*, 5620. (l) Caro, C. F.; Hitchcock, P. B.; Lappert, M. F.; Layh, M. *Chem. Commun.* **1998**, 1297. (m) Lucht, B. L.; Collum, D. B. *Acc. Chem. Res.* **1999**, *32*, 1035. (n) Forbes, G. C.; Kennedy, A. R.; Mulvey, R. E.; Rodger, P. J. A.; Rowlings, R. B. *J. Chem. Soc., Dalton Trans.* **2001**, 14. (o) Zhao, P.; Collum, D. B. *J. Am. Chem. Soc.* **2003**, *125*, 14411. (p) Godenschwager, P. F.; Collum, D. B. *J. Am. Chem. Soc.* **2007**, *129*, 12023. (q) Clarke, C.; Fox, D. J.; Pedersen, D. S.; Warren, S. *Org. Biomol. Chem.* **2009**, *7*, 1329–1336. (r) Armstrong, D. R.; Herd, E.; Graham, D. V.; Hevia, E.; Kennedy, A. R.; Clegg, W.; Russo, L. *J. Chem. Soc., Dalton Trans.* **2008**, 1323–1330.

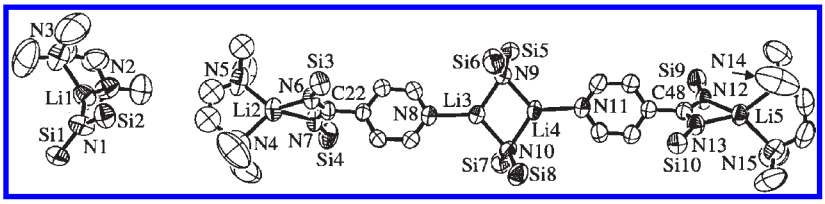

Figure 8. ORTEP diagram of the molecular structure of complex **8** and the $LiN(TMS)_2 \cdot TMEDA$ molecule of crystallization (50% thermal ellipsoids). Methyl groups on silicon and hydrogen atoms are omitted for clarity.

Scheme 4. Plausible Routes for the Formation of Polymers **6** and **7**

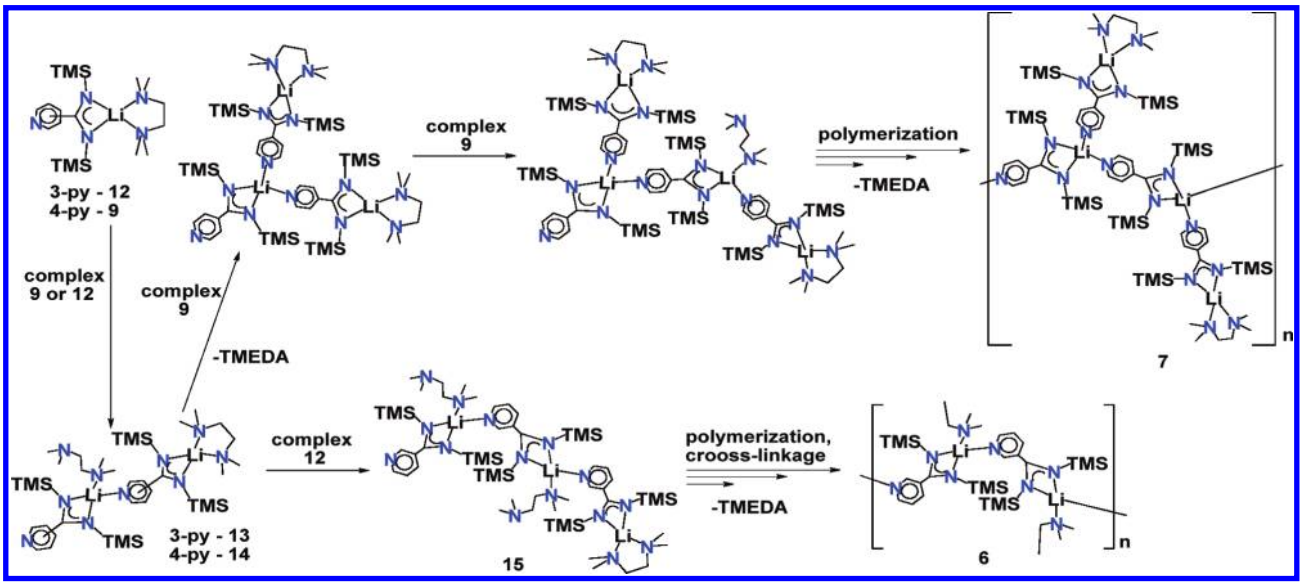

form. It is worth mentioning that in the complex $[C_6F_5NC(2\text{-}C_5H_4N)NSiMe_3]Li \cdot TMEDA$[11] (Figure 9), which can be regarded as complex **5** in which a TMS group was replaced with a sterically similar, electron withdrawing C_6F_5 moiety,[25] the pyridyl nitrogen displaces intramolecularly one of the amidinate nitrogen atoms.

A similar displacement is assumed to be responsible for the unique propylene polymerization properties of bis[*N*, *N*′-bis(trimethylsilyl)-2-pyridyl amidinate] titanium dichloride in comparison to other titanium benzamidinates.[26] The aforementioned steric considerations are likely accountable for the different structures obtained by the 3- and 4-pyridyl amidinates.

Hence, the aggregation of both the monomeric pyridyl amidinates **9** or **12** (Scheme 4) plausibly starts by replacement of one $Li-N_{TMEDA}$ bond with a pyridyl nitrogen from another molecule, while opening the TMEDA chelate, to create the dimers **14** or **13**, respectively. These dimers have two possible ways to continue the polymer growth with consequent enchainment of more monomers: The κ^1 TMEDA can be fully displaced by an additional pyridyl nitrogen, or the κ^2 TMEDA can be opened to a κ^1 mode. For the 4-pyridyl derivative the former path seems to be preferred, and subsequent

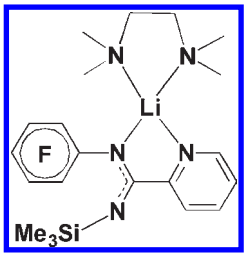

Figure 9. *N*-pentafluorophenyl, *N*′-trimethylsilyl 2-pyridylamidinate Lithium TMEDA.[11]

replacement of the same TMEDA with two pyridyl nitrogens leads to the structure of polymer **7**. The quasi-syndiotactic arrangement of the side chain units is a plausible result of chain-end control of the incoming pyridyl unit.[27]

In the 3-pyridyl amidinate, the consequent opening of the chain-end TMEDA chelate by a newly enchained unit leads to a linear structure that has an amidinate-Li-pyridyl backbone, with κ^1 TMEDA moieties as side chains (complex **15**). Cross-linkage between those chains can occur by replacement of a TMEDA moiety in a certain chain by the free nitrogen of a TMEDA from a neighboring chain, to create the 2D network of complex **6**. In both cases lower solubility of the oligomers and\or removal of free TMEDA by vacuum can divert the equilibrium toward the formation of polymers **6** or **7**. The replacement of TMEDA in $LiNTMS_2 \cdot TMEDA$ by

(25) Hansch, C.; Leo, A.; Hoekman, D. *Exploring QSAR: Hydrophobic, Electronic, and Steric Constants*; American Chemical Society: Washington, DC, 1995; pp 254, 270.

(26) Aharonovich, S.; Kapon, M.; Botoshanski, M.; Eisen, M. S. Substituent Effects in Propylene Polymerization Promoted by Titanium(IV) Amidinates. Proceedings of the 38th International Conference on Coordination Chemistry, Kenes International, Jerusalem, Israel, July 20−25, **2008**; p 369.

(27) Odian, G. *Principles of Polymerization*, 4th ed.; John Wiley & Sons, Inc.: New York, 2004; pp 619−728.

the pyridyl nitrogen of complex **9** and laddering[28] of the $(SiMe_3)_2NLi\cdot\{[4\text{-}C_5H_4NC(NSiMe_3)_2]Li\cdot TMEDA\}$ unit to form the Li−N−Li−N ring can account for the formation of complex **8**.

Conclusions

The introduction of a heterocycle as the carbon substituent in an amidinate system allows the pendant heteroatom to participate in the coordination toward the metal center at the expense of the TMEDA ligand. We have found this TMEDA displacement to occur only with the 3- and 4-pyridyl derivatives, resulting in a 2D (complex **6**) and a linear (complex **7**) coordination polymers, respectively, which have both a κ^2 amidinate-Li-pyridyl backbone. In the furyl and 2-pyridyl complexes, on the other hand, no involvement of the pendant heteroatom was noted, demonstrating the importance of both the Li−E interaction strength and steric factors in the aggregation process. Partial hydrolysis of the unsolvated lithium 3-furyl amidinate **2** generates the Li_2O-amidinate cage complex **4**, in which no $Li-O_{furyl}$ interactions are present. The degradation of the linear polymer **7** to mononuclear lithium 4-pyridyl amidinate TMEDA units can be achieved by its leaching with toluene or by coordination of the pyridyl nitrogen to Li in $LiNTMS_2$.

Experimental Section

General Procedures. All manipulations of air-sensitive materials were carried out with the rigorous exclusion of oxygen and moisture in an oven-dried or flamed Schlenk-type glassware on a dual-manifold Schlenk line, or interfaced to a high vacuum (10^{-5} Torr) line, or in a nitrogen-filled Vacuum Atmospheres glovebox with a medium-capacity recirculator (1−2 ppm O_2). Argon and nitrogen were purified by passage through a MnO oxygen-removal column and a Davison 4 Å molecular sieve column. Analytically pure solvents were distilled under nitrogen from potassium benzophenone ketyl (THF), Na (toluene, TMEDA), and Na/K alloy (ether, hexane, toluene-d_8, THF-d_8). 3-Furonitrile was synthesized in a high yield from 3-furaldehyde (Aldrich) analogously to the preparation of 2-furonitrile,[29] and its melt was distilled from P_4O_{10} under reduced pressure. Lithium bis(trimethylsilyl)amide (Aldrich) was recrystallized from hexane. 3- and 4-Cyanopyridine (Aldrich) were degassed prior to use.

NMR spectra were recorded on Bruker Avance 300 and 500 spectrometers. ^1H and ^{13}C Chemical shifts are referenced to internal solvent resonances and reported relative to tetramethylsilane. ^7Li chemical shifts were referenced to 1 M LiCl in D_2O. The experiments were conducted in Teflon-sealed NMR tubes (J. Young) after preparation of the sample under anaerobic conditions, with dried toluene-d_8 or THF-d_8.

X-ray Crystallographic Measurements. The single crystalline material was immersed in Paratone-N oil and was quickly removed with a capillary tube and mounted on the Kappa CCD diffractometer under a cold stream of nitrogen at 230−240 K. Data collection was performed using monochromatized Mo Kα radiation using ω scans and φ scans to cover the Ewald sphere.[30] Accurate cell parameters were obtained with the amount of indicated reflections (Table 1).[31] The structure was solved by SHELXS97 direct methods,[32] and refined by SHELXL97 program package.[33] The atoms were refined anisotropically. Hydrogens were included using the riding mode. Software used for molecular graphics: ORTEP, TEXRAY Structure Analysis package.[34] Cell parameters and refinement data are presented in Table 1.

$\{[(3\text{-}C_4H_3O)C(NSiMe_3)_2]Li\}_n$ (2). A 8.801 g portion (52.6 mmol) of lithium bis(trimethylsilyl) amide was charged in the glovebox into a swivel frit equipped with two 250 mL flasks, which was then connected to a high vacuum line. A 100 mL portion of hexane was added to the frit, and the resulting solution was cooled to −20 °C. A solution of 4.900 g (52.6 mmol) of the 3-furonitrile in 40 mL of toluene was added dropwise using a syringe, and the mixture was allowed to gradually reach room temperature in the duration of 3 h (dark brown solids start to form above −5 °C). The resulting dark suspension was filtered, and the brown solids were extracted 3 times with 80 mL of toluene at about 50 °C. The extracts were dried in vacuum, and the resulting gray solids were washed with small amounts of cold hexane to receive after drying in vacuum 613 mg (5% yield) of **2**, which was used without further purification.

$[(3\text{-}C_4H_3O)C(NSiMe_3)_2]Li\cdot TMEDA$ (3). A swivel frit equipped with two 25 mL flasks was charged in the glovebox with 250 mg (0.96 mmol) of compound **2**. The frit was connected to a high vacuum line, and 10 mL of hexane was added. The obtained suspension was cooled to 0 °C, and 0.2 mL (1.3 equiv) of TMEDA was added, resulting in the dissolution of most of the solids. The solution was stirred for an additional hour, filtered via the frit to remove the solid impurities, and the volume of the filtrate was gradually reduced by vacuum until precipitation started. The concentrated solution was warmed to room temperature to allow the formation of a clear solution and cooled to −60 °C overnight to yield colorless crystals of the product. The crystals were separated from the mother liquor by decantation, washed carefully with small amount of cold hexane, and dried under vacuum (298 mg, 92% yield). ^1H NMR (300 MHz, Toluene-d_8): δ = 7.23 (dd, J_1 = 1.5 Hz, J_2 = 0.8 Hz, 1H, 5-Furyl C−H), 7.03 (t, J = 1.5 Hz, 1H, 2-Furyl C−H), 6.29 (dd, J_1 = 1.5 Hz, J_2 = 0.8 Hz, 1H, 4-Furyl C−H), 1.98 (s, 12H, CH_3N), 1.80 (s, 4H, CH_2N), 0.10 (s, 18H, CH_3Si); ^{13}C NMR (76.5 MHz, Toluene-d_8): δ = 171.8 (s, 1C, N···C···N), 140.8 (s, 1C, 5-Furyl), 137.5, (s, 1C, 2-Furyl), 130.8 (s, 1C, 3-Furyl), 111.3 (s, 1C, 4-Furyl), 56.5 (s, 2C, CH_2N), 45.6 (s, 4C, CH_3N), 3.4 (s, 6C CH_3Si). Anal. Calcd for $C_{17}H_{37}LiN_4OSi_2$ (376.6): C, 54.22; H, 9.90; N, 14.88. Found: C, 51.00; H, 9.88; N, 13.82.

$\{[(3\text{-}C_4H_3O)C(NSiMe_3)_2]Li\}_6\cdot Li_2O$ (4). A 289 mg portion (1.11 mmol) of compound **2** was charged in the glovebox into a 25 mL Schlenk flask. The flask was connected to a high vacuum line, and its content was mixed with 10 mL of 0.25 mg/mL solution of water in toluene, resulting in a turbid solution. Colorless crystals of the product (48 mg, 30% yield) were separated from this solution after it was stored for 2 weeks at 3 °C. ^1H NMR (500 MHz, Toluene-d_8): δ = 7.30 (dd, J_1 = 1.5 Hz, J_2 = 0.9 Hz, 4H, 5-Furyl C−H), 6.97 (t, J = 1.5 Hz, 4H, 2-Furyl C−H), 6.32 (dd, J_1 = 1.5 Hz, J_2 = 0.9 Hz, 4H, 4-Furyl C−H), 0.12 (s, 72H, CH_3Si); ^{13}C NMR (126.7 MHz, toluene-d_8): δ = 176.4 (s, 1C, N···C···N), 141.5 (s, 1C, 5-Furyl), 138.2 (s, 1C, 2-Furyl), 129.0 (s, 1C, 3-Furyl), 111.2 (s, 1C, 4-Furyl), 3.3 (s, 24C, CH_3Si). ^7Li NMR (194.3 MHz, toluene-d_8): δ = 2.25.

(28) (a) Armstrong, D. R.; Barr, D.; Clegg, W.; Mulvey, R. E.; Reed, D.; Snaith, R.; Wade, K. *J. Chem. Soc., Chem. Commun.* **1986**, 869. (b) Gregory, K.; Schleyer, P. v. R.; Snaith, R. *Adv. Inorg. Chem.* **1991**, *37*, 47. (c) Mulvey, R. *E. Chem. Soc. Rev.* **1991**, *20*, 167. (d) Mulvey, R. E. *Chem. Soc. Rev.* **1998**, *27*, 339. (e) Downard, A.; Chivers, T. *Eur. J. Inorg. Chem.* **2001**, 2193.

(29) Talukdar, S.; Hsu, J. L.; Chou, T. C.; Fang, J. M. *Tetrahedron Lett.* **2001**, *42*, 1103–1105.

(30) *Kappa CCD Server Software*; Nonius BV: Delft, The Netherlands, 1997.

(31) Otwinowski, Z.; Minor, W. *Methods Enzymol.* **1997**, *276*, 307–326.

(32) Sheldrick, G. M. *Acta Crystallogr., Sect. A: Found. Crystallogr.* **1990**, *A46*, 467–473.

(33) Sheldrick, G. M. *SHELXL97, Program for the Refinement of Crystal Structures*; University of Gottingen: Gottingen, Germany, 1997.

(34) *ORTEP, TEXRAY Structure Analysis Package*; Molecular Structure Corporation, MSC: 3200 Research Forest Drive, The Woodlands, TX, 1999.

Anal. Calcd for $C_{44}H_{84}Li_6N_8O_5Si_8$ (1071.5): C, 49.32; H, 7.90; N, 10.46. Found: C, 44.80; H, 7.79; N, 11.21.

General Procedure for Syntheses of the Pyridyl Amidinates 6 and 7. A 1.941 g portion (11.6 mmol) of lithium bis(trimethylsilyl) amide was charged in the glovebox into a swivel frit equipped with two 100 mL flasks. After the frit was connected to a high vacuum line, 30 mL of toluene was added, and the resulting solution was cooled to −10 °C. A solution of 1.206 g (11.6 mmol) of the corresponding cyanopyridine in 9 mL of toluene was added dropwise using a syringe. The cooling bath was removed, and the resulting suspension was stirred at room temperature for 2 h. TMEDA (5 equivalents) was then added, and the obtained turbid solution was stirred for 5 min at 40 °C. The almost clear solution was then filtered while hot, and volatiles were evaporated from the filtrate until turbidity was noted. The concentrated filtrate was cooled to −50 °C, and the formed solids were separated from the mother liquor by fast filtration, washed with small amounts of cold hexane, and dried under vacuum to give 3.478 g of complex **6** (91% yield) or 3.252 g of complex **7** (85% yield).

{[3-C$_5$H$_4$NC(NSiMe$_3$)$_2$]Li·0.5TMEDA}$_n$ (6). ^{1}H NMR (300 MHz, THF-d_8): δ = 8.32 (dd, J_1 = 4.9 Hz, J_2 = 2.1 Hz, 2H, 6-py C−H), 8.25 (dd, J_2 = 2.1 Hz, J_3 = 0.8 Hz, 2H, 2-py C−H), 7.29 (dt, J_4 = 7.7 Hz, J_2 = 2.1 Hz, 2H, 4-py C−H), 7.10 (ddd, J_4 = 7.7 Hz, J_1 = 4.9 Hz, J_3 = 0.8 Hz, 2H, 3-py C−H), 3.58 (s, OC*H*D), 2.31 (s, 4H, CH_2N), 2.15 (s, 12H, CH_3N), 1.72 (s, OCD_2CHD), −0.32 (s, 36H, CH_3Si); ^{13}C NMR (76.5 MHz, THF-d_8): δ = 175.0 (s, 2C, CN_2), 147.8 (s, 2C, 6-py), 147.6 (s, 2C, 2-py), 143.6 (s, 2C, 3-py), 132.8 (s, 2C, 4-py), 132.1 (s, 2C, 5-py), 67.4 (q, OCD_2CD_2), 58.9 (s, 2C, CH_2N), 46.2 (s, 4C, CH_3N), 25.3 (q, OCD_2CD_2), 3.0 (s, 12C CH_3Si). Anal. Calcd for $C_{23}H_{52}Li_2N_8Si_4$ (659.1): C, 54.67; H, 9.18; N, 17.00. Found: C, 51.36; H, 8.51; N, 15.74. (The combustion with these compounds even in the presence of V_2O_5 is not complete because of the formation of carbide compounds.)

({[4-C$_5$H$_4$NC(NSiMe$_3$)$_2$]Li·[4-C$_5$H$_4$NC(NSiMe$_3$)$_2$]Li·TMEDA})$_n$ (7). ^{1}H NMR (300 MHz, THF-d_8): δ = 8.52 (dd, J_1 = 4.2 Hz, J_2 = 1.6 Hz, 4H, 2-py C−H), 7.17 (dd, J_1 = 4.2 Hz, J_2 = 1.6 Hz, 4H, 3-py C−H), 3.58 (s, OC*H*D), 2.31 (s, 4H, CH_2N), 2.15 (s, 12H, CH_3N), 1.72 (s, OCD_2CHD), −0.32 (s, 36H, CH_3Si); ^{13}C NMR (76.5 MHz, THF-d_8): δ = 175.0 (s, 2C, CN_2), 147.8 (s, 2C, 6-py), 147.6 (s, 2C, 2-py), 143.6 (s, 2C, 3-py), 132.8 (s, 2C, 4-py), 132.1 (s, 2C, 5-py), 67.4 (q, OCD_2CD_2), 58.9 (s, 2C, CH_2N), 46.2 (s, 4C, CH_3N), 25.3 (q, OCD_2CD_2), 3.0 (s, 12C CH_3Si). Anal. Calcd for $C_{23}H_{52}Li_2N_8Si_4$ (659.1): C, 54.67; H, 9.18; N, 17.00. Found: C, 53.36; H, 7.94; N, 16.96.

{[N(SiMe$_3$)$_2$]Li·{[4-C$_5$H$_4$NC(NSiMe$_3$)$_2$]Li·TMEDA}}$_2$·{[N(SiMe$_3$)$_2$]Li·TMEDA} (8). A 1.126 g portion (1.7 mmol) of complex **7** was dissolved in 10 mL of toluene and 10 mL of TMEDA, and a solution of 0.737 g (4.4 mmol) of lithium bis(trimethylsilyl) amide in 10 mL of toluene was injected to the frit. The mixture was stirred for 1 h, filtered, and volatiles were evaporated from the filtrate until turbidity was noted. The concentrated solution was cooled to −30 °C, and the resulting colorless crystals were separated by decantation and washed twice with small amounts of cold hexane to give 1.808 g (76% yield) of complex **8**. ^{1}H NMR (300 MHz, Toluene-d_8): δ = 8.86 (d, J = 6.1 Hz, 4H, 2-py C−H), 7.09 (d, J = 6.1 Hz, 4H, 3-py C−H), 1.94 (br. s, 36H, CH_3N), 1.77 (br. s, 12H, CH_2N), 0.45 (br. s, 36H, μ_2-N[Si(CH$_3$)$_3$]$_2$), 0.35 (br. s, 18H, N[Si(CH$_3$)$_3$]$_2$), −0.05 (s, 36H, C[NSi(CH$_3$)$_3$]$_2$); ^{13}C NMR (76.5 MHz, Toluene-d_8): δ = 174.8 (s, 2C, CN_2), 156.2 (s, 2C, 4-py), 149.4 (s, 4C, 2-py), 122.1 (s, 4C, 3-py), 56.3 (br. s, 6C, CH_2N), 45.5 (br. s, 12C, CH_3N), 6.6 (s, 18C, N[Si(CH$_3$)$_3$]$_2$), 3.1 (br. s, 12C, C[NSi(CH$_3$)$_3$]$_2$). Anal. Calcd for $C_{60}H_{146}Li_5N_{15}Si_{10}$ (1393.52): C, 51.70; H, 10.56; N, 15.08. Found: C, 51.81; H, 10.17; N, 14.48.

Degradation of Polymer 7 by Toluene and THF under NMR Monitoring. A 66 mg portion (0.1 mmol) of complex **7** was weighed inside the glovebox into a J. Young NMR tube, which was cooled to liquid nitrogen temperature and pumped-down. About 1 mL of toluene-d_8 was vacuum-transferred into the NMR tube, which was then filled with argon, and heated to room temperature. The tube was shaken for an hour and kept aside for additional 15 min to allow solids to precipitate. The filtrate was decanted to a separate tube where its NMR data was recorded. ^{1}H NMR (500 MHz, Toluene-d_8): δ = 8.53 (dd, J_1 = 4.2 Hz, J_2 = 1.5 Hz, 2H, 2-py C−H), 6.97 (dd, J_1 = 4.2 Hz, J_2 = 1.5 Hz, 2H, 3-py C−H), 2.00 (s, 12H, CH_3N), 1.88 (s, 4H, CH_2N), −0.01 (s, 18H, CH_3Si); ^{13}C NMR (126.8 MHz, Toluene-d_8): δ = 176.3 (s, 1C, CN_2), 154.1 (s, 1C, 4-py), 149.8 (s, 2C, 2-py), 121.1 (s, 2C, 3-py), 56.8 (s, 2C, CH_2N), 45.6 (s, 4C, CH_3N), 3.2 (s, 3C, CH_3Si).

The NMR tube with the white solids (vide supra) was washed with two 0.6 mL aliquots of toluene, and interfaced to a high vacuum line where all of the remaining toluene was evacuated. About 0.6 mL of THF-d_8 were then vacuum-transferred into the tube, giving a transparent solution. ^{1}H NMR (500 MHz, THF-d_8): δ = 8.56 (dd, J_1 = 4.5 Hz, J_2 = 1.5 Hz, 2H, 2-py C−H), 7.73 (dd, J_1 = 4.5 Hz, J_2 = 1.5 Hz, 2H, 3-py C−H), 3.58 (s, OC*H*D), 1.72 (s, OCD_2CHD), −0.07 (s, 18H, CH_3Si); ^{13}C NMR (126.8 MHz, THF-d_8): δ = 160.2 (s, 1C, CN_2), 150.4 (s, 1C, 4-py), 149.2 (s, 2C, 2-py), 120.9 (s, 2C, 3-py), 67.4 (q, OCD_2CD_2), 25.3 (q, OCD_2CD_2), 2.0 (s, 9C CH_3Si).

Acknowledgment. This research was supported by the U.S.A.-Israel Binational Science Foundation under contract 2008283. S.A. thanks Mr. Raymond Rosen for the fellowship.

Supporting Information Available: X-ray crystallographic data in CIF files for compounds **3**, **4**, **6**−**8**. This material is available free of charge via the Internet at http://pubs.acs.org.